

Computational approaches for clean energy materials

Stephan Lany

National Renewable Energy
Laboratory

Golden, CO 80401

- Defect graph neural networks
- Equilibria with interacting defects
- Interface structure prediction

Collaborations

Anuj Goyal (NREL, IITH)

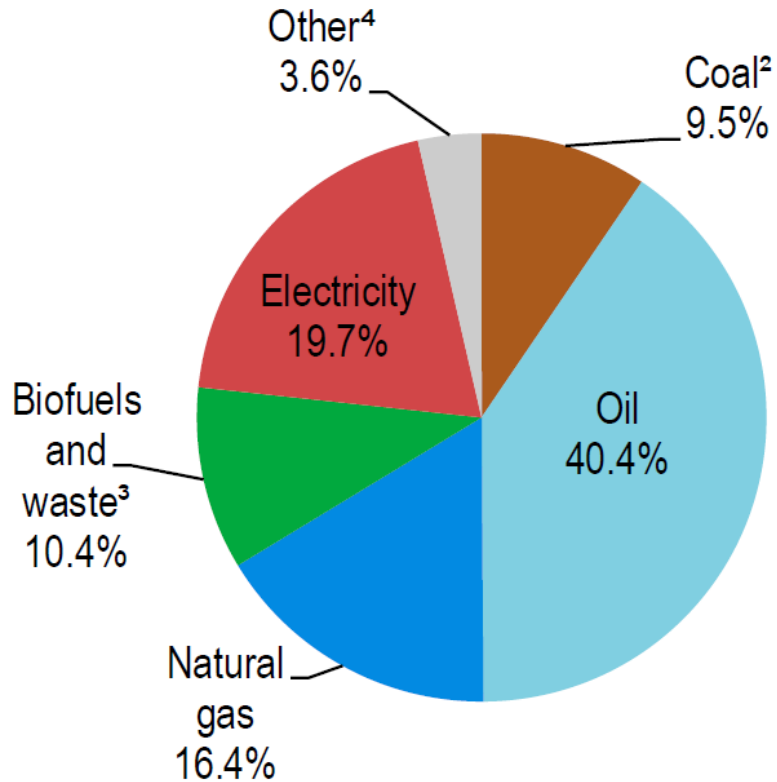
Matt Witman, Tony McDaniel (SNL), Tadashi Ogitsu (LLNL)

Michael Sanders, Ryan O'Hayre (Mines)

Abhishek Sharan (NREL, KU), N. Singh, D. Krasikov (First Solar), Marco Nardone (BGSU)

Energy transition

2019 world final energy consumption by source



20% electricity / 80% fuels

Key World Energy Statistics 2021, IEA report

2050 Energy Needs (average power)

- Current infrastructure 58,000 GW
- Trend extrapolation **32,000 GW**
- Total electrification 12,000 GW

Kurtz *et al*, Revisiting the Terawatt Challenge, MRS Bulletin 2020

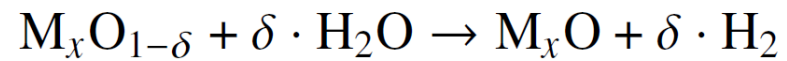
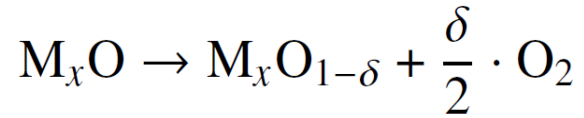
2022	P_{cap} (GW)	f_{cap} (%)	P_{av} (GW)
Hydro	1400	40	560
Wind	900	35	320
Solar (PV)	1000	15	150
Total	3400		1,030

Renewable Capacity Statistics 2023, IRENA report

add/yr	P_{cap} (GW)	f_{cap} (%)	P_{av} (GW)
Hydro	30	40	12
Wind	80	35	28
Solar (PV)	220	15	33
Total	340		63

Renewables 2022, IEA report

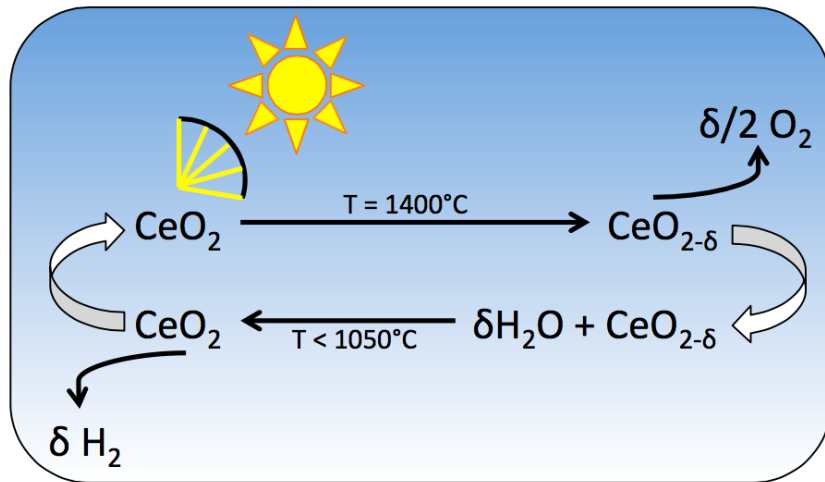
Non-electricity solar fuels: Thermochemical Hydrogen



Reduction (solar heat)

Oxidation (H_2 production)

Ideal gas law (H_2 , O_2 , H_2O)



(1) Materials Discovery

Down-selection of candidate materials
Broad screening of materials databases

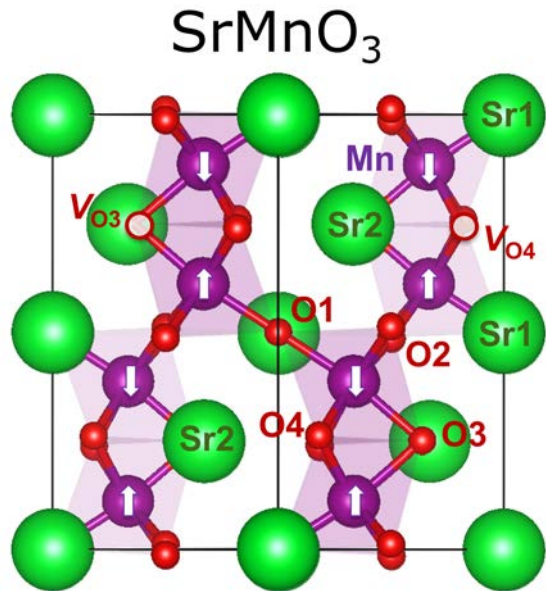
(2) Quantitative and mechanistic models

Specific materials systems
Understand the underlying physics
Assess potential and limitations

Supercell calculations

- O vacancy formation energy

$$\Delta H_D^{\text{ref}} = E_D - E_H + \mu_O^{\text{ref}}$$

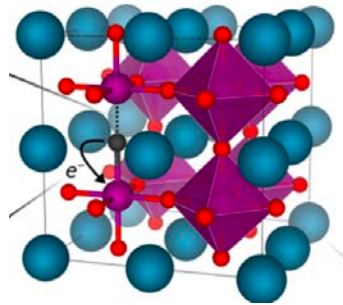


	Mn-O-Mn (°)	ΔH_D^{ref} (eV)
O1	174.3	3.27
O2	171.1	3.27
O3	82.0	2.33
O4	82.1	2.35

(1) Screening and discovery ML models for defects

Phenomenological models can be quite successful

Deml *et al*, JPCL 2015
Wexler *et al*, JACS 2021



Linear Model works well for ABO₃ perovskites:

$$0.1 \Sigma E_b - 1.5 V_r + 0.4 E_g - 55.8 E_{\text{hull}} + 0.4 \text{ (eV)}$$

↑ Crystal bond dissociation
 ↑ Crystal reduction
 ↑ Band gap
 ↑ Stability
 ← features

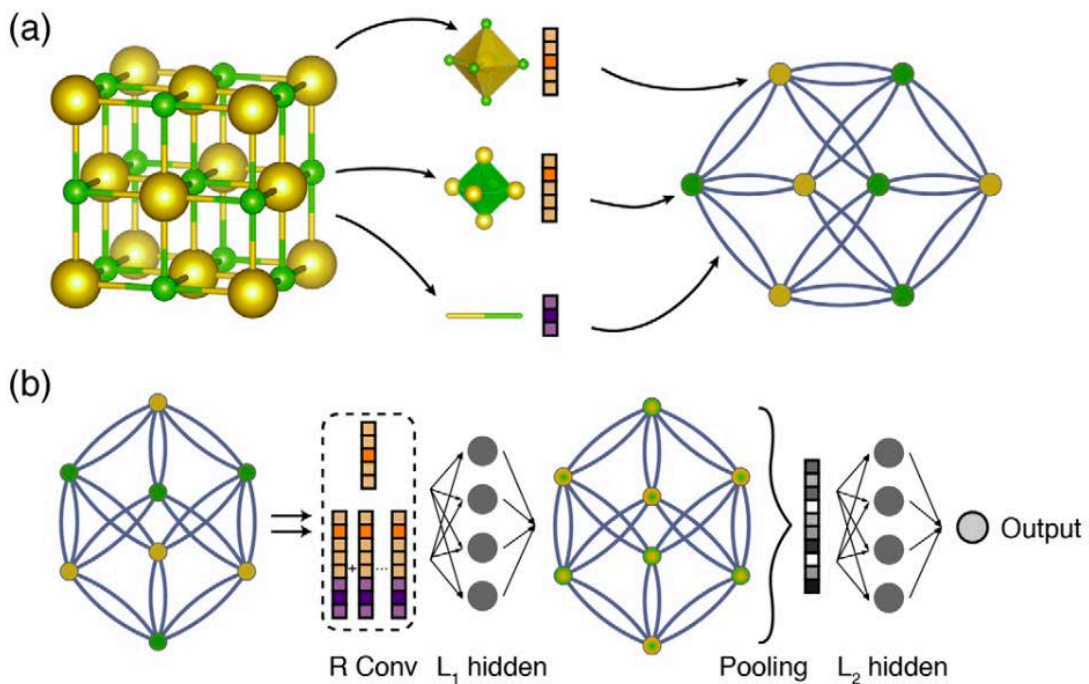
- Model limitations to specific chemistries and/or structure types
- Limited scaling of accuracy of regression-based approaches
- Explicit structure dependence needed to differentiate symmetry sites

Defect Graph Neural Network

Explicit structure dependence via graph neural networks

- Crystal Graph Convolutional Neural Networks
- Automated feature extraction

Xie and Grossman, PRL (2018)



Crystal structure -> energy

- Need defect structure
- Accuracy of energy differences?

$$\text{DFT: } \Delta H_D = E_{\text{DFT}}(\mathbf{X}_D) - E_{\text{DFT}}(\mathbf{X}_H) + \mu_{\text{O}}^{\text{ref}}$$

supercells
~100 atoms



$$\text{ML using only host structure: } \Delta \hat{H}_D = f_{\text{GNN}}(\mathbf{X}_h, i'; \theta)$$



- Encode the graph (step $t = 0$):

$$\mathbf{v}_1^{t=0} = \{r_{\text{O}}, \chi_{\text{O}}, \dots, s_1\}$$

Accuracy boosting, site-specific inputs (i.e. oxidation state)

- Convolutions ($t = 1 \dots T$)

$$\mathbf{v}_i^{(t+1)} = g \left(\mathbf{v}_i^{(t)} + \sum_j \sigma \left(\mathbf{z}_{ij}^{(t)} \mathbf{W}_1^{(t)} + \mathbf{b}_1^{(t)} \right) \odot g \left(\mathbf{z}_{ij}^{(t)} \mathbf{W}_2^{(t)} + \mathbf{b}_2^{(t)} \right) \right)$$

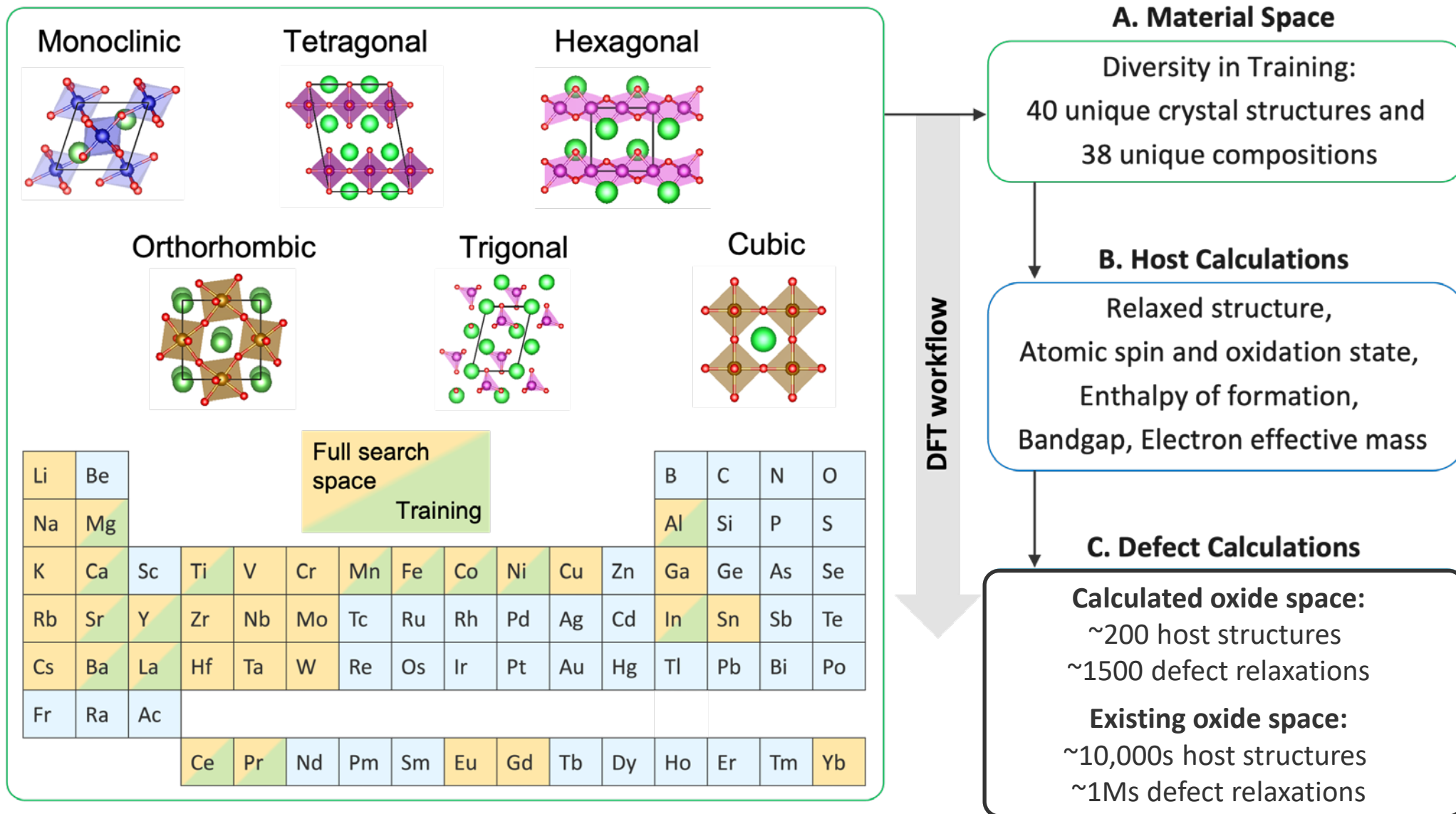
- Node-level pooling

$$\mathbf{v}_d = g \left((\mathbf{v}_{i'}^{(T)} \oplus \mathbf{v}_g) \cdot \mathbf{W} + \mathbf{b} \right)$$

➤ Extract defect feature vector
➤ Use host's global properties,
 $\mathbf{v}_g = \{E_g, m^*, \Delta H_f\}$

Structurally and compositionally diverse training data

First-principles DFT workflow is robust but time consuming (using NRELMatDB hosts)



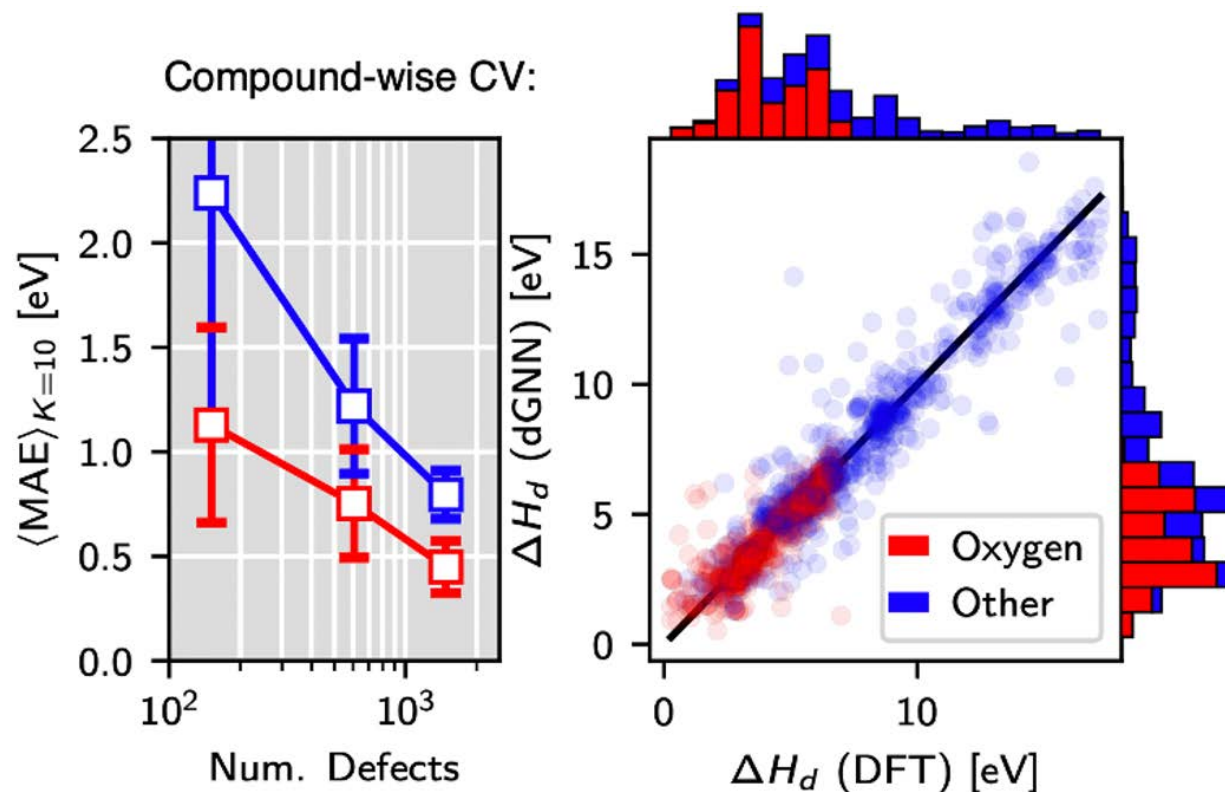
Benchmarking

Encoding strategies

- Element only: Crystal structure and atomic type
- Full: Additional local (s_i) and global (v_g) properties

Cross-validation

- Defect-wise vs compound-wise



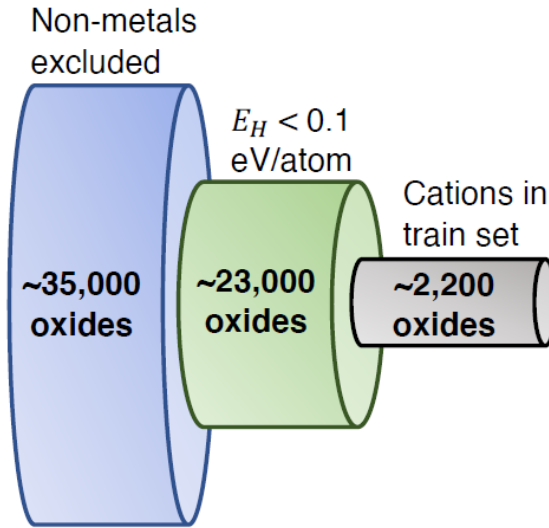
Model Encoding Type		Element only (v_e)		DFT only (s_i, v_g)		Full (v_e, s_i, v_g)		Continuous (v'_e, s'_i, v_g)	
		ΔH_d^O	$\Delta H_d^{\text{Other}}$	ΔH_d^O	$\Delta H_d^{\text{Other}}$	ΔH_d^O	$\Delta H_d^{\text{Other}}$	ΔH_d^O	$\Delta H_d^{\text{Other}}$
Defect-wise CV:	$\langle \text{MAE}^Y \rangle_K$	0.37	0.85	0.44	0.82	0.30	0.65	0.31	0.66
	$\sigma_K(\text{MAE}^Y)$	(0.08)	(0.11)	(0.06)	(0.12)	(0.03)	(0.08)	(0.03)	(0.05)
Compound-wise CV:	$\langle \text{MAE}^Y \rangle_K$	0.52	0.96	0.58	1.13	0.45	0.79	0.49	0.78
	$\sigma_K(\text{MAE}^Y)$	(0.16)	(0.18)	(0.17)	(0.20)	(0.12)	(0.12)	(0.19)	(0.19)

Materials Project screening

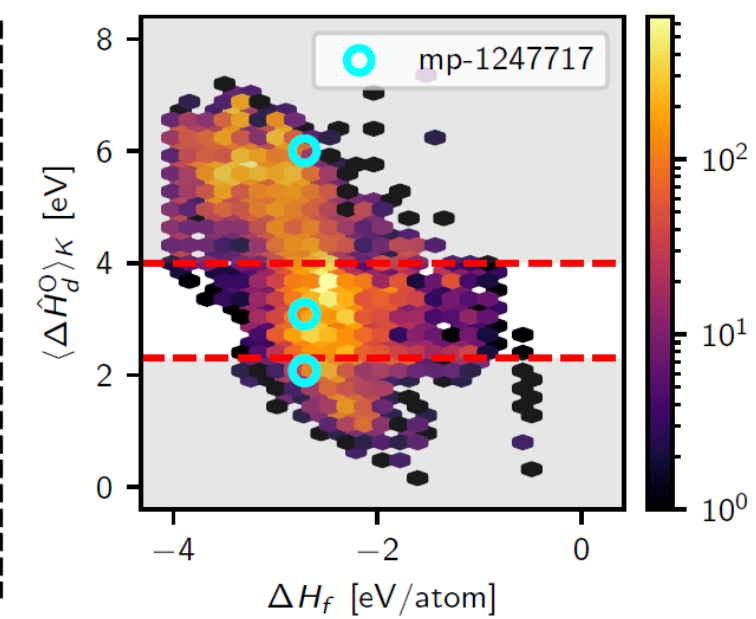
Co-design of defects and stability for water-splitting

Metric	Requirement
Frac. of defects w/ $\Delta H_d^O > 2.3$ eV	$x_{\min} = 1$
Frac. of defects w/ $\Delta H_d^O \in [2.3, 4.0]$ eV	$x_{\text{rng}} > 0$
P_{O_2} operating conditions for STCH	$\Delta\mu'_{O_2}$
P_{O_2} where host's GC energy above hull $< X$	$\Delta\mu_{O_2}^{\phi_H < X}$
Host stability criteria (ranges intersect)	$\Delta\mu_{O_2}^{\phi_H < X} \cap \Delta\mu'_{O_2}$

(a) Oxides to screen



(b) Predict all defects



753 formulas (80 training)	197 formulas (48 training)	114 formulas (33 training)	34 formulas (17 training)	16 formulas (11 training)	9 formulas (9 training)
<ul style="list-style-type: none"> $x_{\min,1} = 1$ $x_{\text{rng},1} > 0$ $E_H < 0.1$ 	<ul style="list-style-type: none"> $x_{\min,1} = 1$ $x_{\text{rng},1} > 0$ $\Delta\mu_O^{\phi_H < 0.1}$ 	<ul style="list-style-type: none"> $x_{\min,2} = 1$ $x_{\text{rng},2} > 0$ $\Delta\mu_O^{\phi_H < 0.1}$ 	<ul style="list-style-type: none"> $x_{\min,3} = 1$ $x_{\text{rng},3} > 0$ $\Delta\mu_O^{\phi_H < 0.05}$ 	<ul style="list-style-type: none"> $x_{\min,3} = 1$ $x_{\text{rng},3} > 0$ $\Delta\mu_O^{\phi_H = 0}$ 	<ul style="list-style-type: none"> $x_{\min,3} = 1$ $x_{\text{rng},3} = 1$ $\Delta\mu_O^{\phi_H = 0}$
	Sr ₆ Ti ₃ FeO ₁₄ (mp-1645141)	La ₂ MnCoO ₆ (mp-19208)	BaSr(FeO ₂) ₄ (mp-1228024)	Ba ₅ SrLa ₂ Fe ₄ O ₁₅ (mp-698793)	Ba ₃ In ₂ O ₆ (mp-20352)

High-throughput thermodynamics

Witman, Goyal, Ogitsu, McDaniel, Lany
Nat Comp Sci (2023)

Thermodynamic analysis

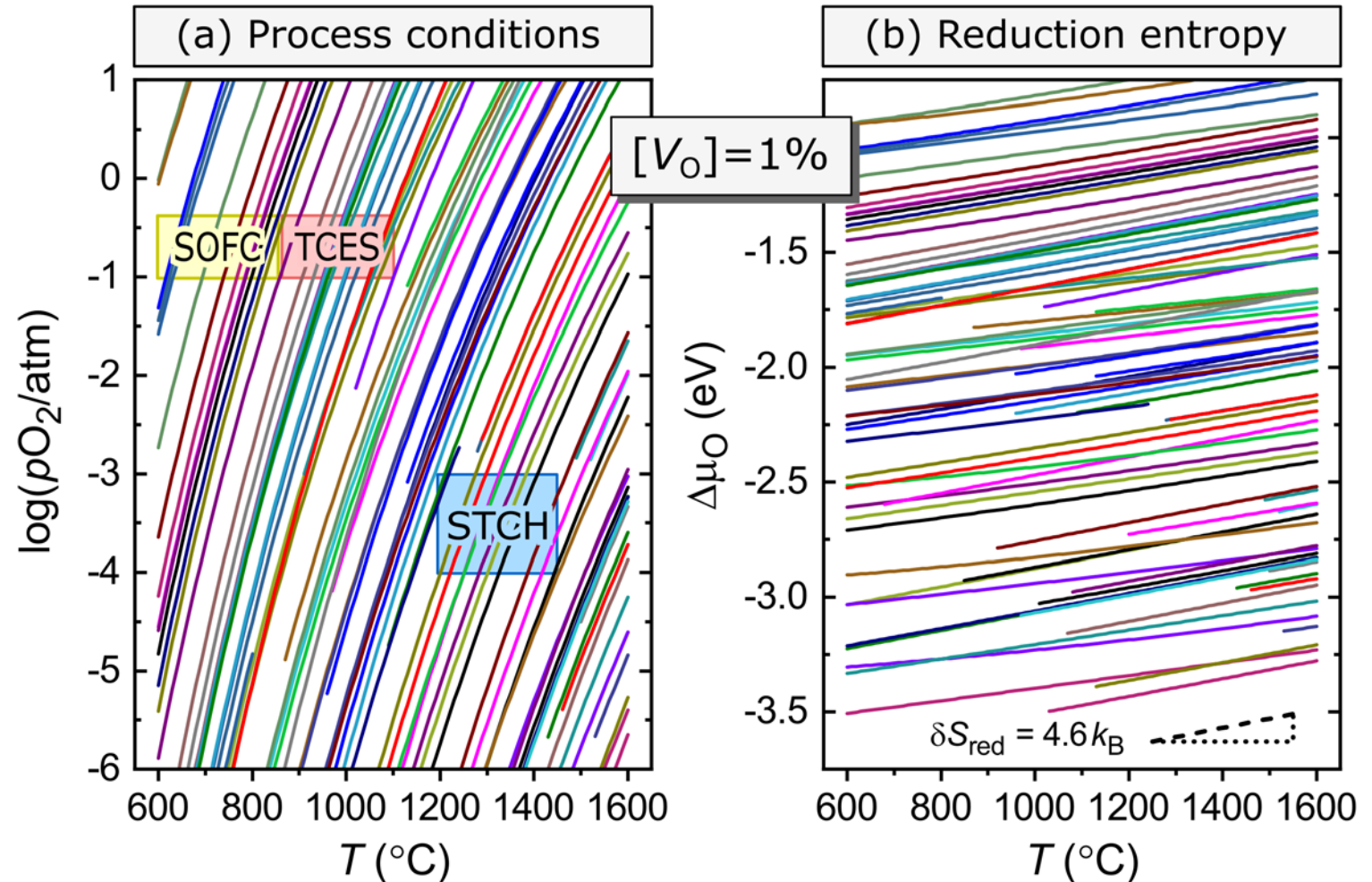
- Sum over non-equivalent sites

$$[V_O] = \sum_i g_i \frac{\exp[-(\Delta H_{V_O,i} + \Delta\mu_O)/k_B T]}{1 + \exp[-(\Delta H_{V_O,i} + \Delta\mu_O)/k_B T]}$$

- Inversion of $\Delta\mu_O \rightarrow [V_O]$ relationship
- Ideal gas law for (pO_2, T) diagrams
- Entropy analysis

$$\frac{\partial}{\partial T} \Delta\mu_O(T) = \frac{\partial}{\partial \delta} \Delta S^{\text{red}}$$

SL, JCP 2018

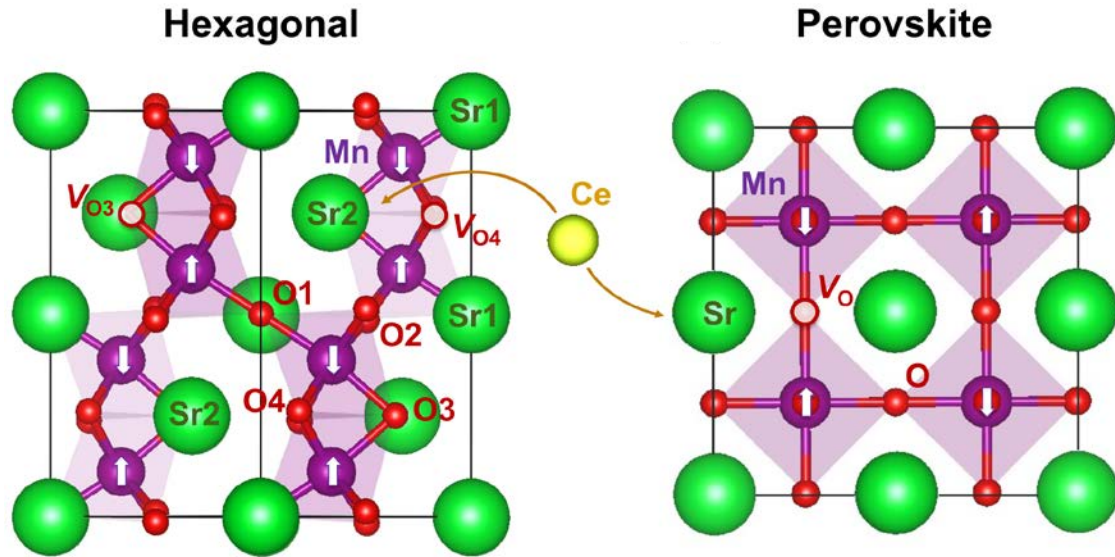


Quantitative and mechanistic models

VASP-SCAN+U

$$U_{\text{Mn-d}} = 2 \text{ eV}$$

$$U_{\text{Ce-f}} = 1 \text{ eV}$$



hex	$d_{\text{Mn-O}}$ (Å)	Mn-O-Mn (°)	ΔH_D^{ref} (eV)
O1/O2	1.89-1.92	82	2.37
O3/O4	1.87-1.89	171-174	3.30
perov			
O1	1.90	180	2.04



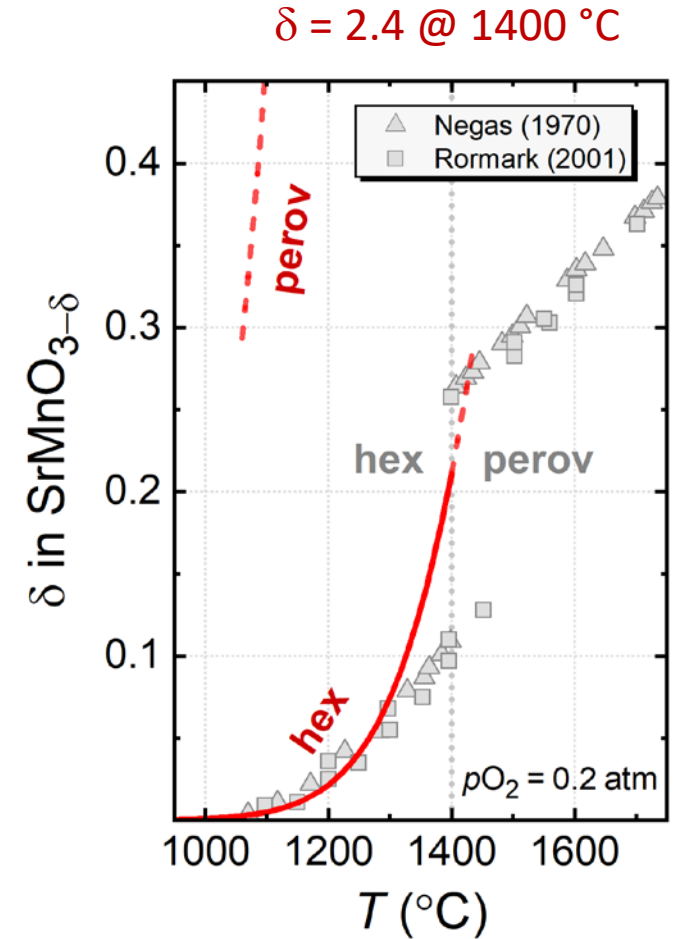
HydroGEN seedling

School of Mines

R. O'Hayre

M. Sanders

Role of repulsive defect interactions?



$$\Delta H_D = \Delta H_D^{\text{ref}} + \Delta \mu_{\text{O}}$$

$$[V_{\text{O}}] = \frac{\exp(-\Delta H_D/k_B T)}{1 + \exp(-\Delta H_D/k_B T)}$$

Modeling interacting defects

cm CHEMISTRY OF MATERIALS

2022

pubs.acs.org/cm

Article

Redox Defect Thermochemistry of FeAl_2O_4 Hercynite in Water Splitting from First-Principles Methods

Samantha L. Millican, Jacob M. Clary, Charles B. Musgrave,* and Stephan Lany*

cm CHEMISTRY OF MATERIALS

2022

pubs.acs.org/cm

Article

Predicting Oxygen Off-Stoichiometry and Hydrogen Incorporation in Complex Perovskite Oxides

Samantha L. Millican, Ann M. Deml, Meagan Papac, Andriy Zakutayev, Ryan O'Hayre, Aaron M. Holder, Charles B. Musgrave,* and Vladan Stevanović*

npj | computational materials

2023

www.nature.com/npjcompumats

ARTICLE OPEN

Check for updates

Accurate prediction of oxygen vacancy concentration with disordered A-site cations in high-entropy perovskite oxides

Jiyun Park¹, Boyuan Xu², Jie Pan³, Dawei Zhang⁴, Stephan Lany⁵, Xingbo Liu⁶, Jian Luo^{4,7} and Yue Qi^{1,8}

Attractive defect interactions

- Electrostatic or strain energies
- Defect pair/complex binding energy
- Law-of-mass-action

Disorder and solid solutions

- Distribution of defect energies

Repulsive defect interactions

- Concentration-dependent formation energy

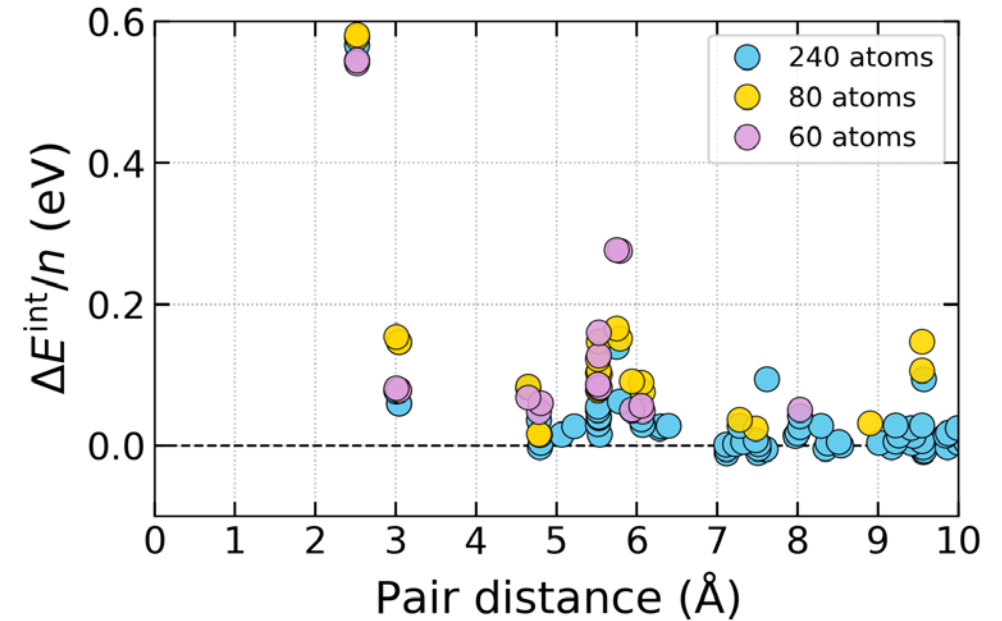
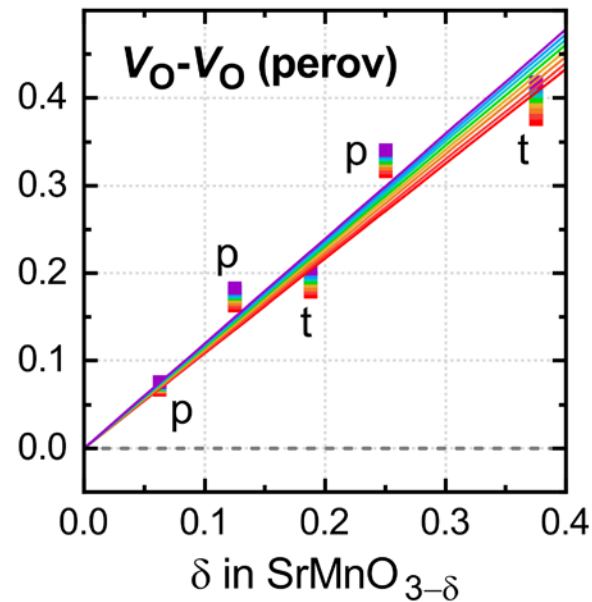
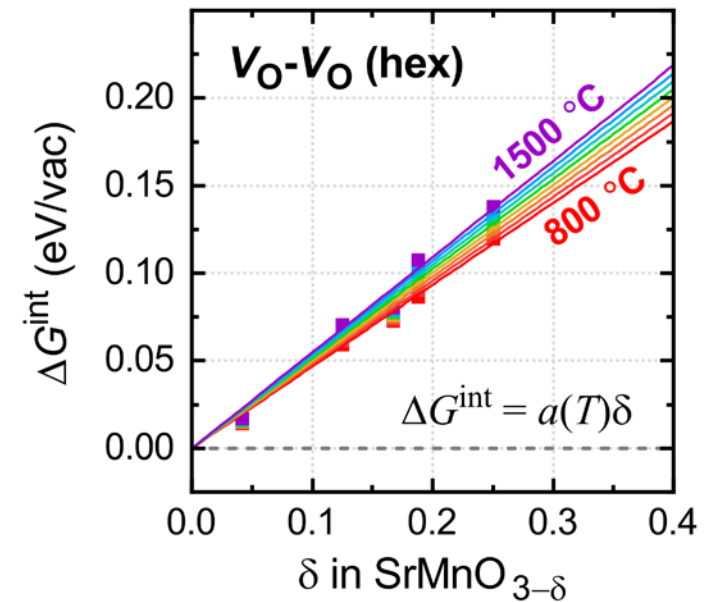
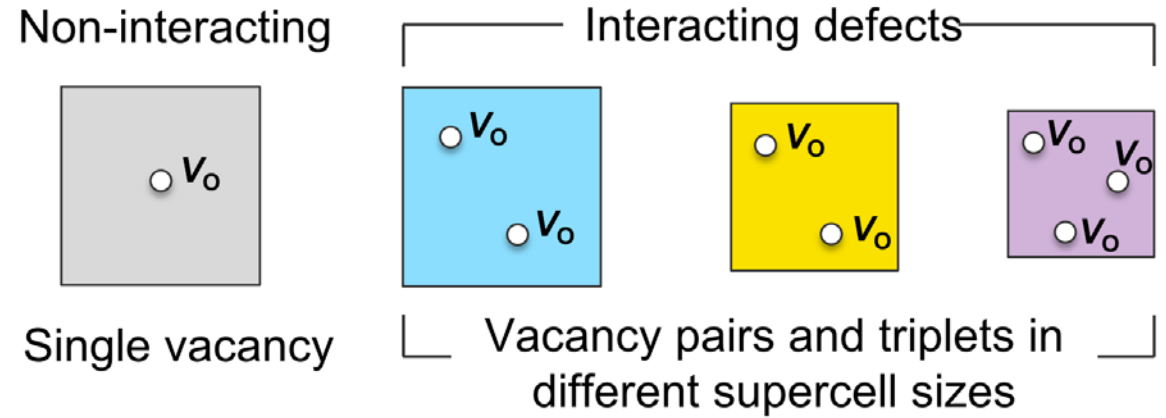
Defect model

Free energy of defect interaction

$$\Delta E_i^{\text{int}} = \Delta H_{D,i}(nV_O) - n \times \Delta H_D(V_O)$$

$$\Delta G^{\text{int}} = -\frac{k_B T}{n} \ln \sum_i \left(g_i \exp \left(-\Delta E_i^{\text{int}} / k_B T \right) \right)$$

$$\Delta G^{\text{int}}(T) = (a_0 + a_1 T) \delta \quad \text{parameterization}$$



SrMnO₃ reduction

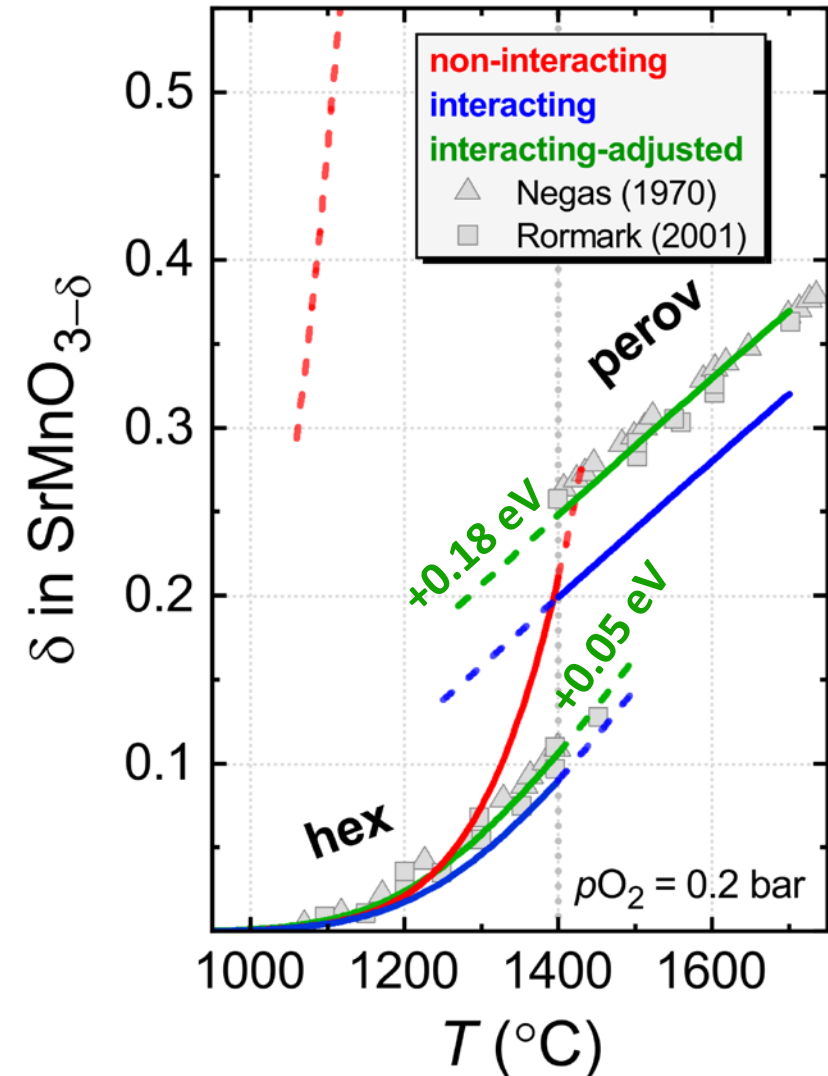
Interacting defect model

- δ moderately underestimated in both phases
- Very good description of T -dependence
- Slight adjustment of ΔH_D yields perfect agreement for all T

Hexagonal-perovskite phase transition

- $\Delta E_{\text{poly}} = 0.16$ eV/fu in SCAN+U
 $\Delta G^{\text{tot}} = 0.13$ eV/fu
- Possible additional contributions:
 - vibrational free energies and ZPE
 - polymorph energies beyond DFT

$$\Delta G^{\text{tot}} = f_d \left(x_V (\Delta H_D + \Delta G_D^{\text{int}}) + k_B T (x_V \ln(x_V) + (1 - x_V) \ln(1 - x_V)) \right)$$



Ce alloying in $\text{Sr}_{1-x}\text{Ce}_x\text{MnO}_{3-\delta}$

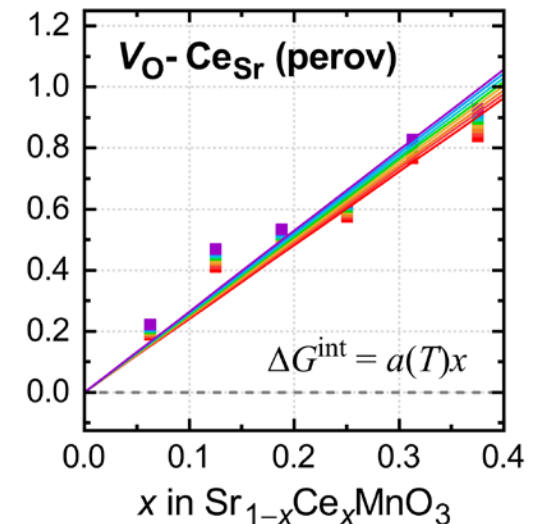
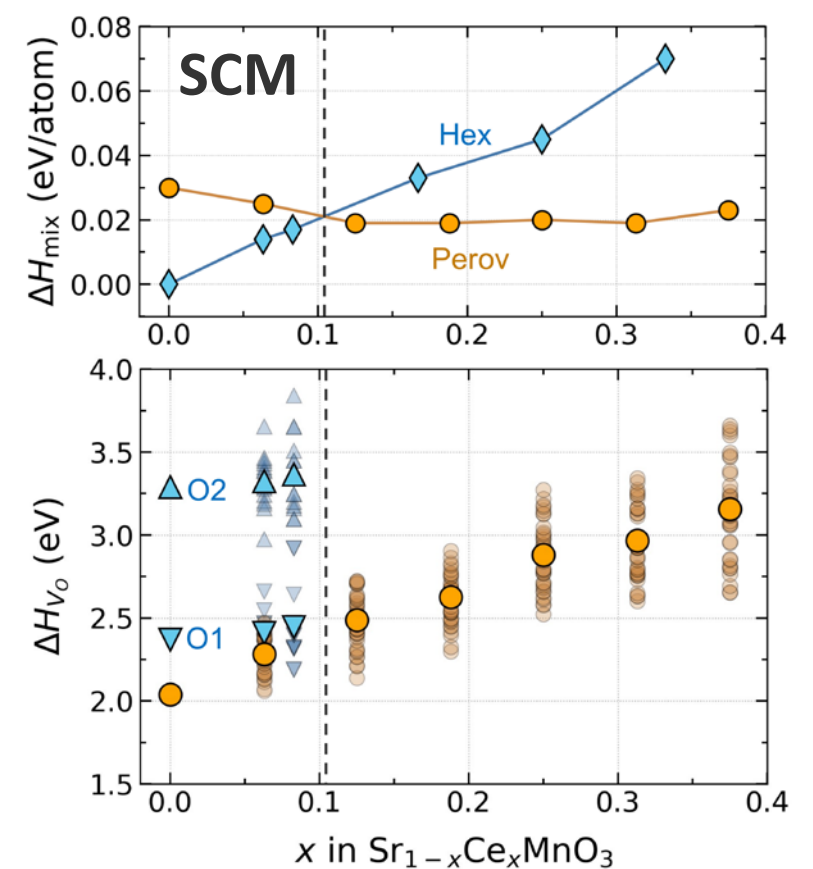
Mixing enthalpy

- Positive ΔH_{mix} as expected for solid solution
- $x = 1$: CeMnO_3 is unstable wrt $\text{CeO}_2 + \text{MnO}$
- Hexagonal-Perovskite transition at $x = 0.1$ (experimentally at $x = 0.05$)

O vacancy formation energies

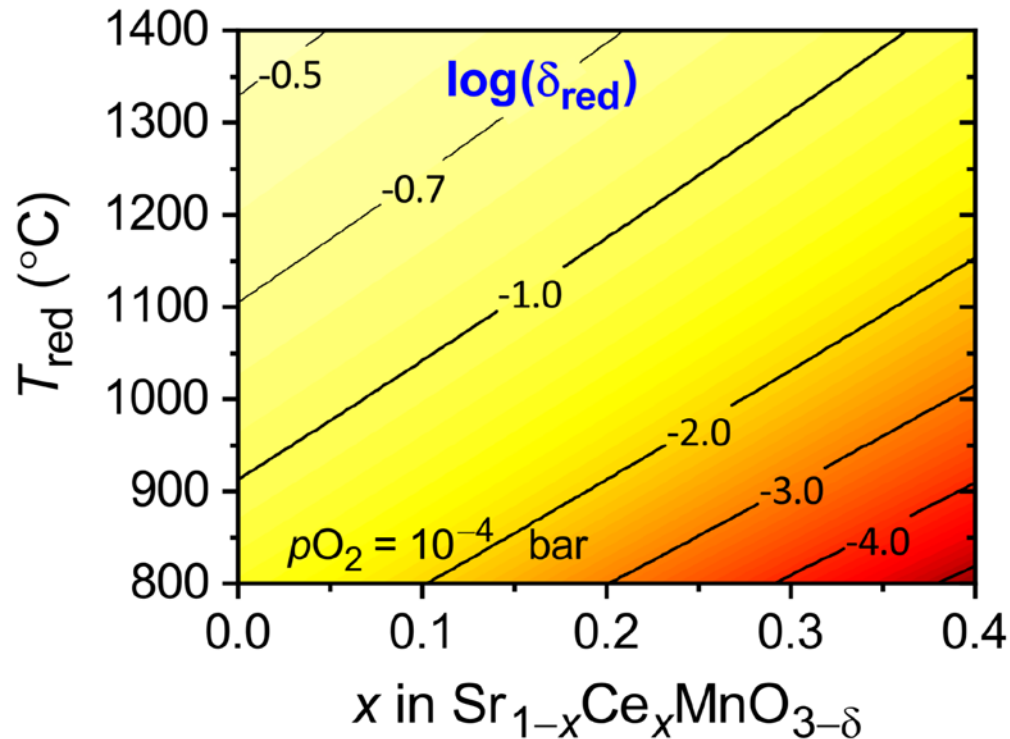
- Strong x dependence
- Superposition of defect interactions:

$$\Delta G^{\text{int}}(T) = (a_0 + a_1 T) \delta + (a_0' + a_1' T) x_{\text{Ce}}$$

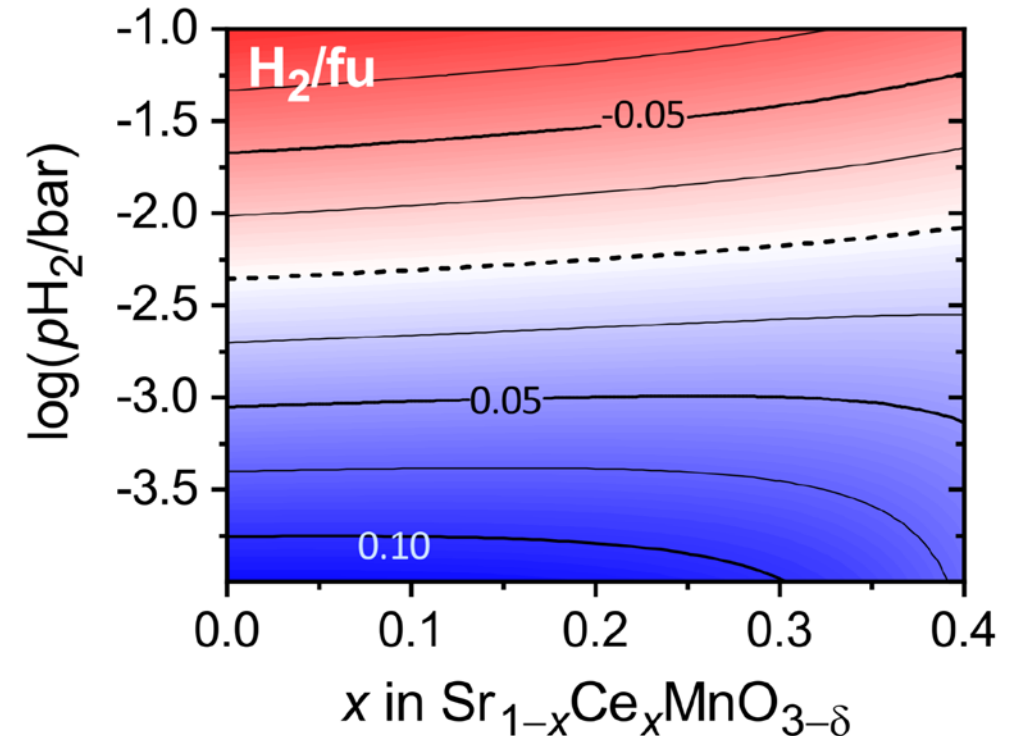


SCM reduction and H₂

- δ decreases with Ce fraction
- Near quantitative agreement with experiment [Bergeson-Keller et al, Ene. Tech. \(2022\)](#)

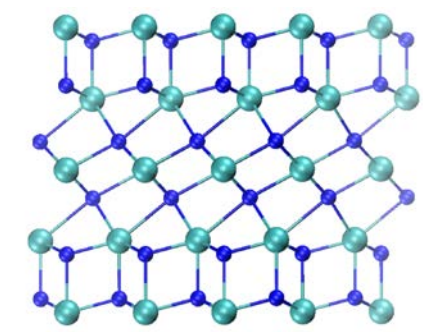
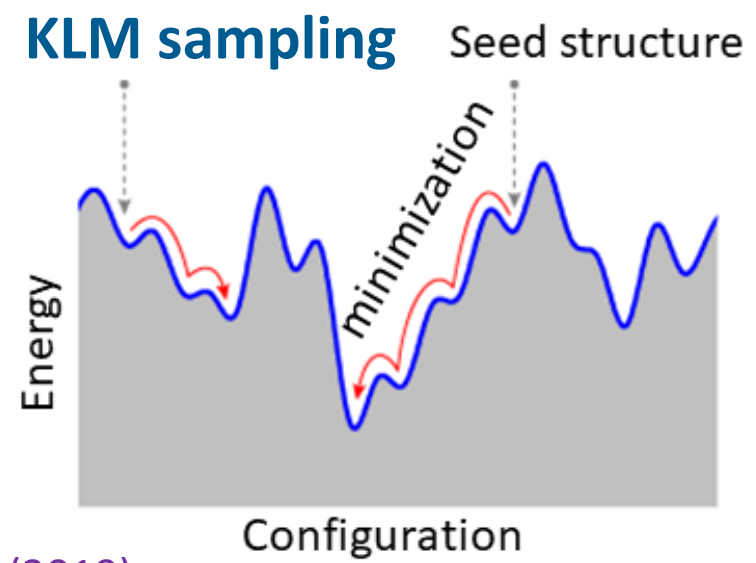
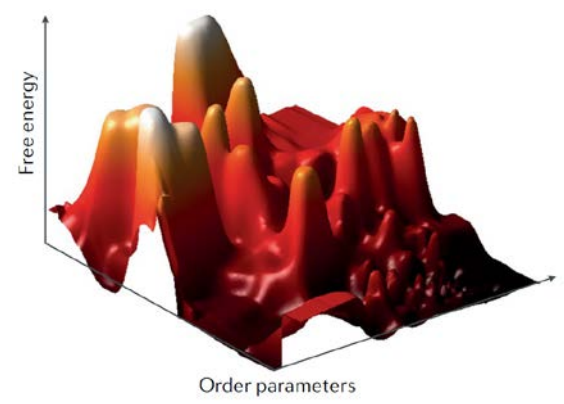


- Reduction: $T = 1400$ °C, $p\text{O}_2 = 10^{-4}$ atm
- Oxidation: $T = 850$ °C, $p\text{H}_2\text{O} = 1$ atm
- Ideal gas law: $\text{H}_2 + \text{O}_2 \leftrightarrow \text{H}_2\text{O}$
- Water splitting only under dilute $\text{H}_2:\text{H}_2\text{O}$
 $p\text{H}_2 < 10^{-2}$ atm
- Increasing $p\text{H}_2$ threshold with x_{Ce}

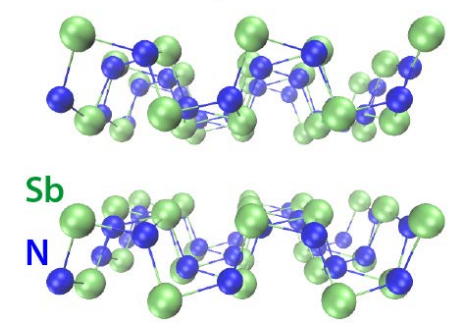


Materials Discovery – structure prediction

New metastable binary nitrides



Ce₃N₄ (sg 166)
 $E_g = 2.15$ eV

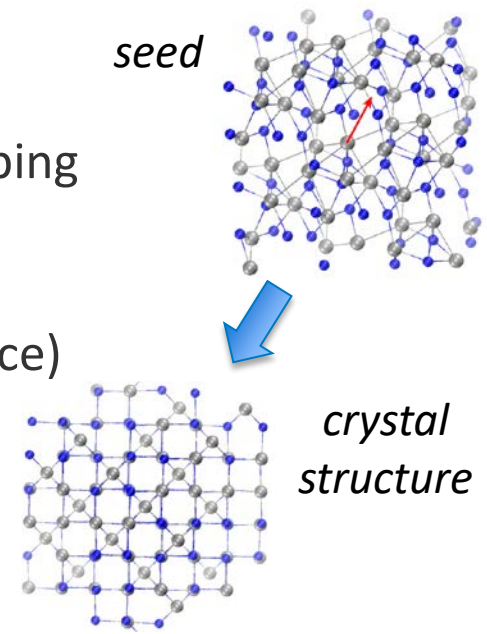


SbN (sg 29)
 $E_g = 2.21$ eV

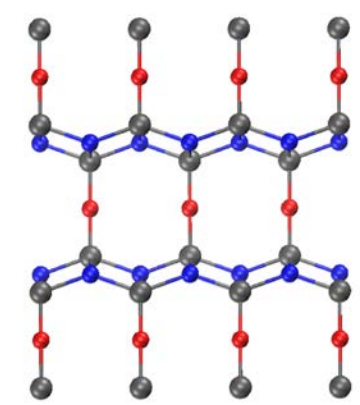
Oganov, Pickard, Zhu, Needs, Nature Reviews Materials 4, 331 (2019)

Kinetically limited minimization (KLM)

- Hybrid random search and basin hopping
- DFT total energy (VASP-PAW)
- Metastable materials
- Reduction of phase space (min distance)
- Applications
 - ternary nitrides
 - oxynitrides



Oxynitrides



Ti₂ON₂ (sg 139)
 $E_g = 1.74$ eV

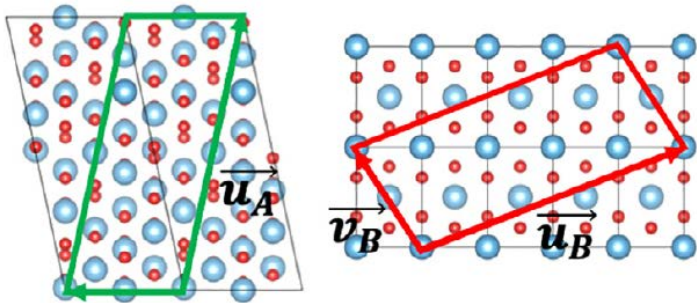
Sharan, SL, JCP (2021)
Chen, SL, et al, Cell Reports (2022)

Structure prediction for interfaces?

Construction of interfaces structures (literature)

coincidence site lattice
(CSL)

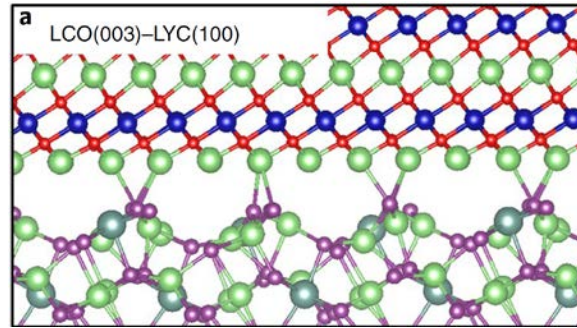
Zur, McGill, JAP (1984)



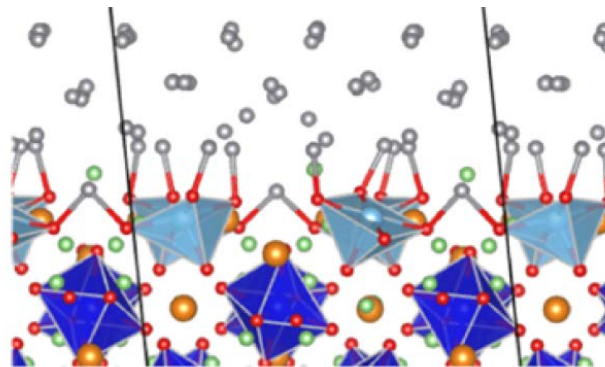
$$\vec{v}_A \quad \begin{bmatrix} 1 & 1 \\ -1 & 0 \end{bmatrix} \quad \begin{bmatrix} 4 & 1 \\ -1 & 1 \end{bmatrix}$$

Gao *et al*, Sci Bull (2019)

free-surface joint
(free surfaces, translation)



Zahiri *et al*, Nat Mater (2021)

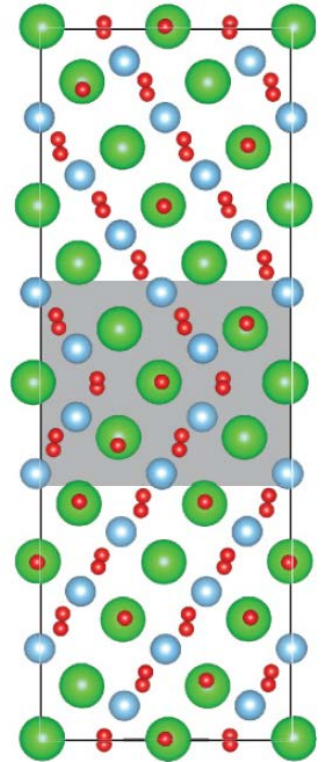


Gao *et al*, ACS Appl Mat Int (2020)

structure sampling

SrTiO₃
grain
boundary

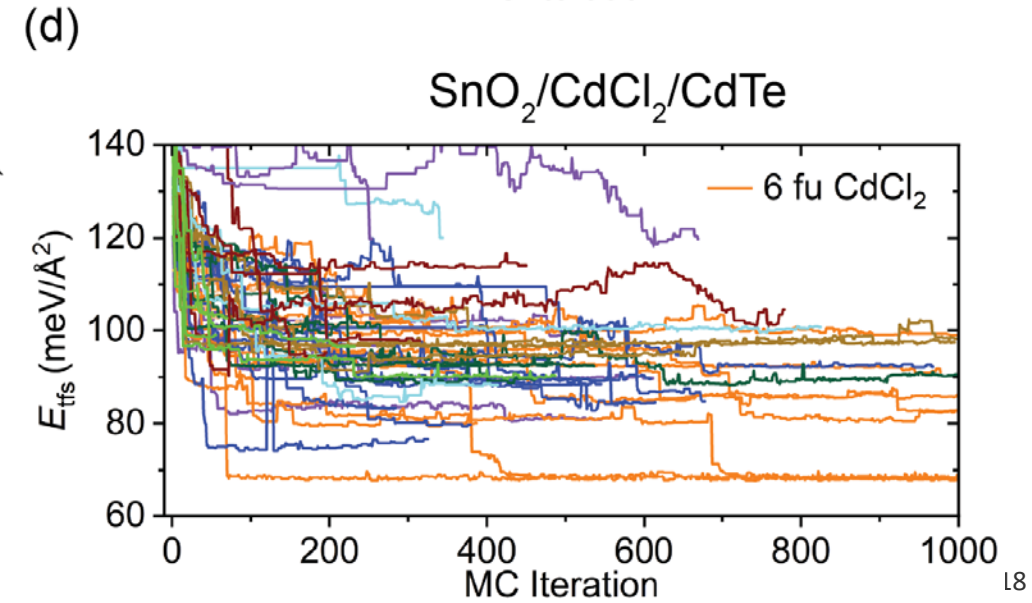
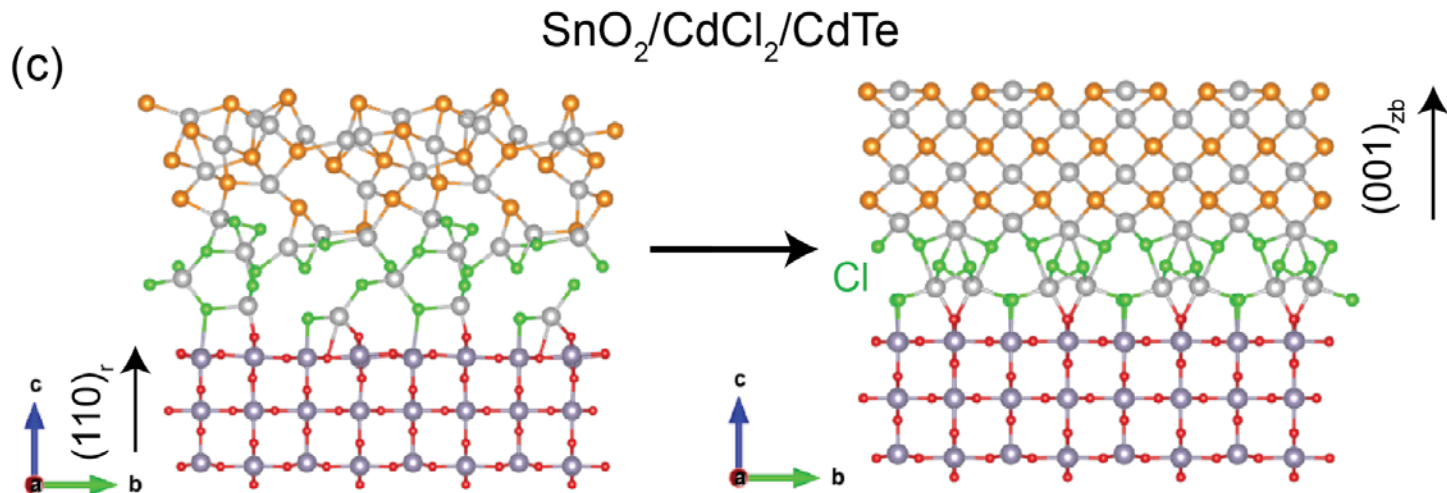
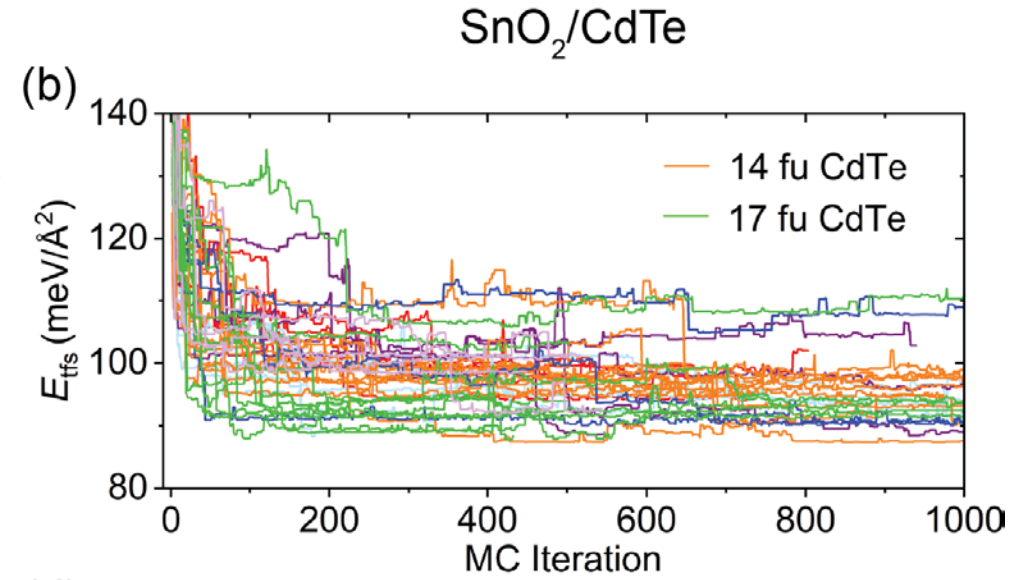
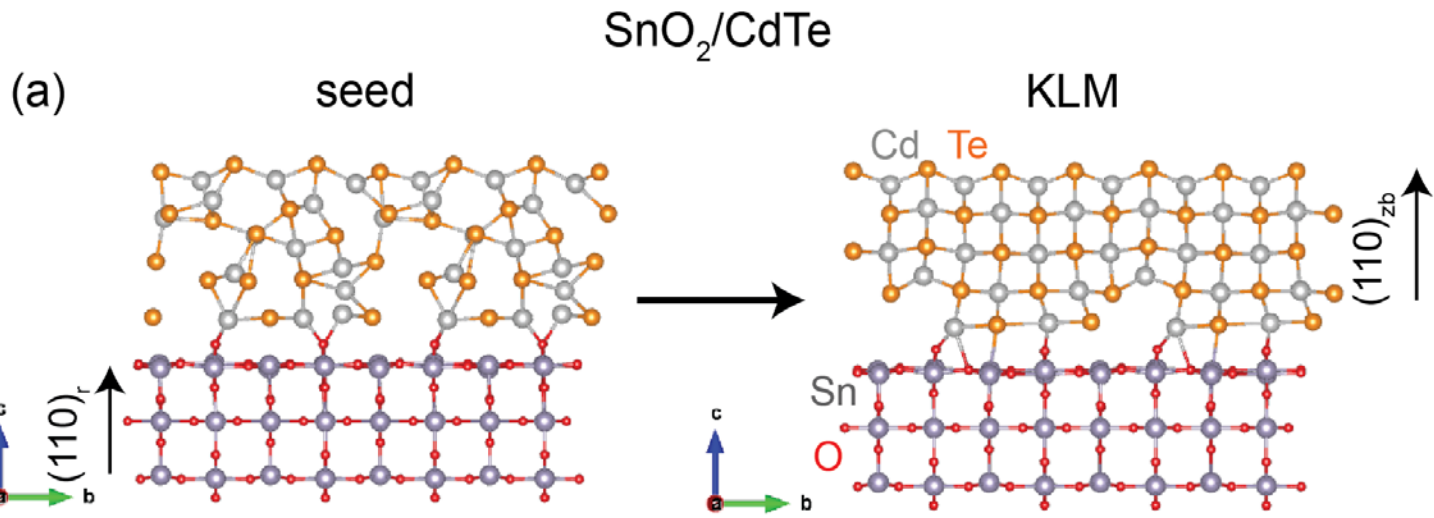
randomization
region



Schusteritsch, Pickard, PRB (2014)

Interface structure prediction: SnO₂/CdTe

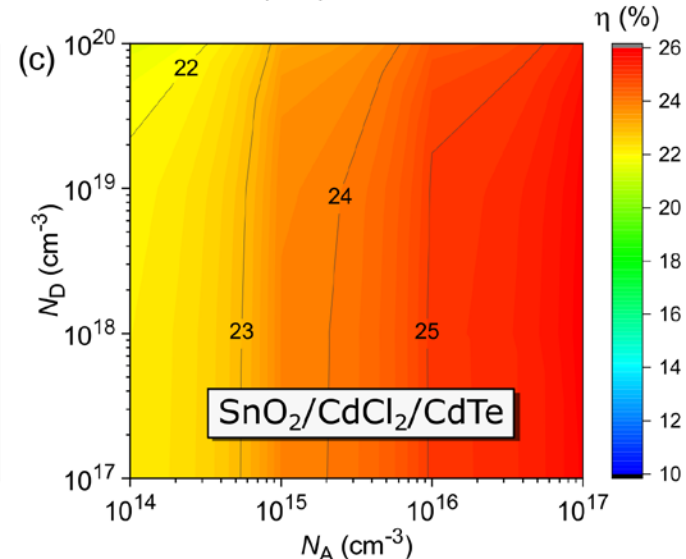
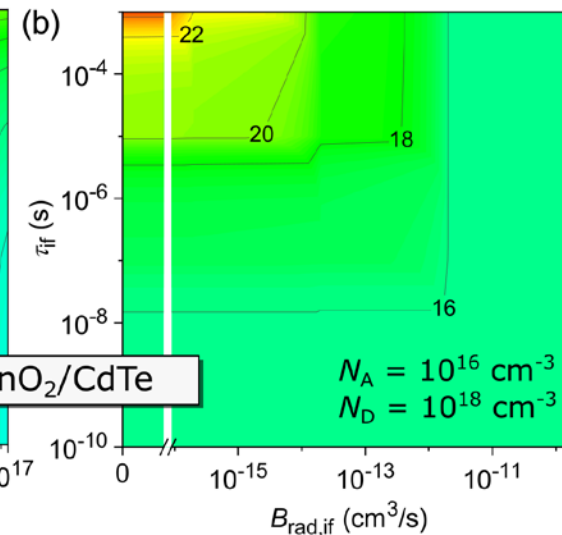
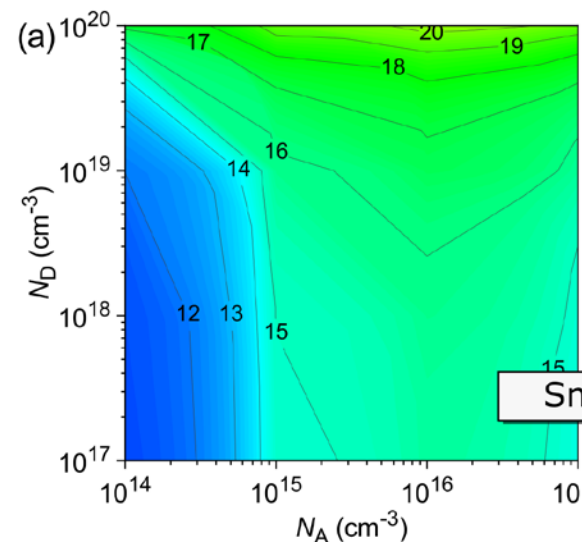
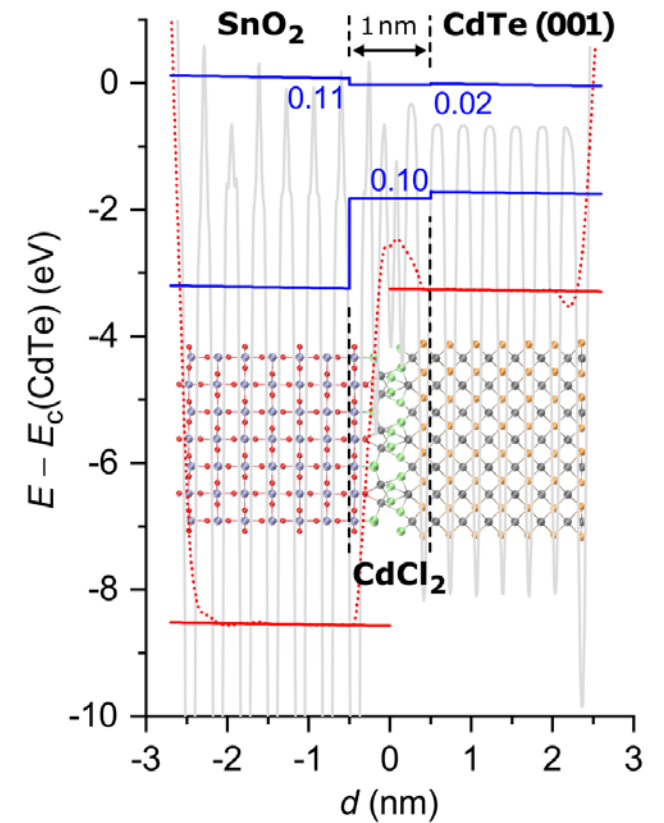
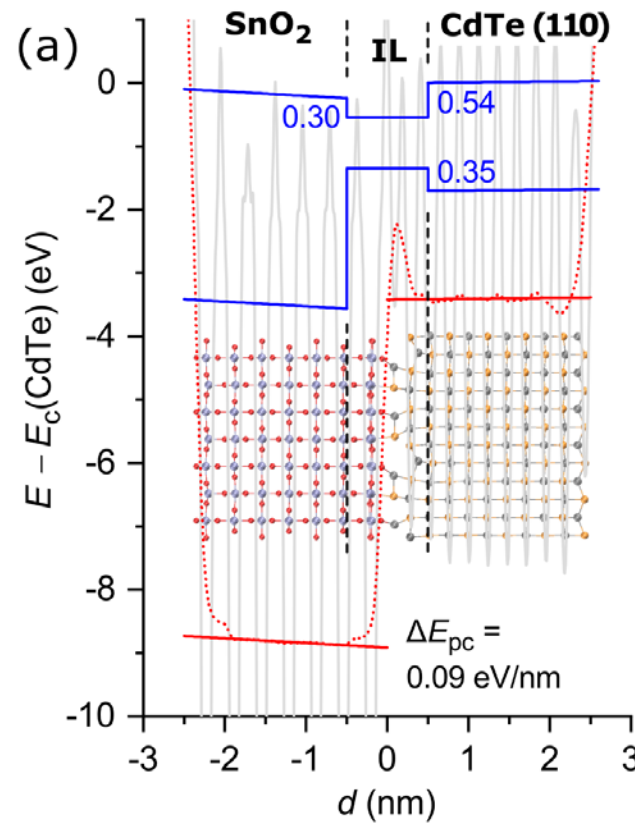
Sharan *et al*, SL,
Appl Phys Rev (2022)



From first-principles to device modeling

- Band gap corrected calculation
- Definition of 1 nm interface layer
- Band alignment data enters device modeling
- CdCl₂ interlayer changes device behavior
- η approaches SQ limit

Sharan *et al*, SL, Appl Phys Rev (2022)



Energy Transition

- Need for direct, non-electricity renewable fuels (H₂)

Machine learning of defect formation energies

- dGNN approach uses crystal structure of defect-free system
- Database screening and targeted experimental and theoretical studies for STCH (NREL, Sandia, LLNL)

M.D. Witman, A. Goyal, T. Ogitsu, A.H. McDaniel, S. Lany,
Nature Comp. Sci. 3, 675 (2023)

Thermochemical equilibria with interacting defects

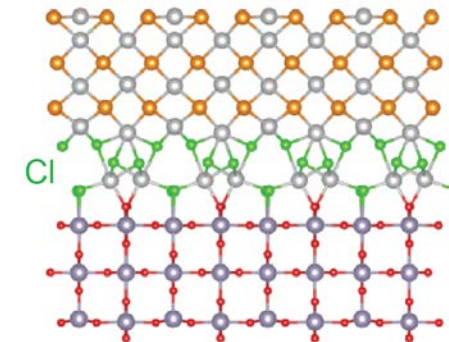
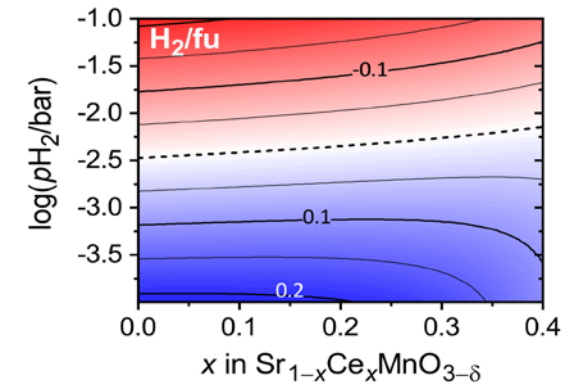
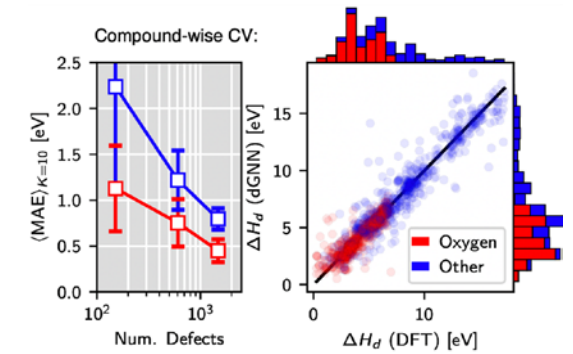
- Free energy of defect interaction $\Delta G_D^{\text{int}}(\delta, x, T)$ for Sr_{1-x}Ce_xMnO_{3-δ}
- Thermodynamic modeling of H₂ yield vs pH₂

A. Goyal, M.D. Sanders, R.P. O'Hayre, S. Lany,
PRX Energy 3, 013008 (2024)

Interface structure predictions

- Opportunities in “Interface Discovery”
- Atomically thin interlayers to connect otherwise incompatible materials

A. Sharan, M. Nardone, D. Krasikov, N. Singh, S. Lany,
Appl. Phys. Rev. 9, 041411 (2022)



Thank you

www.nrel.gov

NREL/PR-5K00-89707

This work was performed in part at the National Renewable Energy Laboratory, operated by Alliance for Sustainable Energy, LLC, for the U.S. Department of Energy (DOE) under Contract No. DE-AC36-08GO28308. Funding provided by the U.S. Department of Energy, Office of Energy Efficiency and Renewable Energy, Hydrogen and Fuel Cell Technologies Office. The views expressed in the article do not necessarily represent the views of the DOE or the U.S. Government. The U.S. Government retains and the publisher, by accepting the article for publication, acknowledges that the U.S. Government retains a nonexclusive, paid-up, irrevocable, worldwide license to publish or reproduce the published form of this work, or allow others to do so, for U.S. Government purposes.

